Polymer Nanocomposite Dielectrics – The Role of the Interface

M. Roy, J.K. Nelson, R.K. MacCrone, L.S. Schadler
Rensselaer Polytechnic Institute
110 8th Street,
Troy, NY 12180, USA

C.W. Reed
116 Woodhaven Dr.,
Scotia, NY 12302, USA

R. Keefe and **W. Zenger**
Electric Power Research Institute
3412 Hillview Ave,
Palo Alto, CA 94303, USA

ABSTRACT

The incorporation of silica nanoparticles into polyethylene increased the breakdown strength and voltage endurance significantly compared to the incorporation of micron scale fillers. In addition, dielectric spectroscopy showed a decrease in dielectric permittivity for the nanocomposite over the base polymer, and changes in the space charge distribution and dynamics have been documented. The most significant difference between micron scale and nanoscale fillers is the tremendous increase in interfacial area in nanocomposites. Because the interfacial region (interaction zone) is likely to be pivotal in controlling properties, the bonding between the silica and polyethylene was characterized using Fourier Transformed Infra-red (FTIR) spectroscopy, Electron Paramagnetic Resonance (EPR), and X-ray Photoelectron Spectroscopy (XPS) The picture which is emerging suggests that the enhanced interfacial zone, in addition to particle-polymer bonding, plays a very important role in determining the dielectric behavior of nanocomposites.

Index Terms — **Nanodielectrics, polyethylene, interface, dielectric strength, polymer nanocomposites, advanced materials, electrical insulation.**

1 INTRODUCTION

NANOPARTICLE-FILLED polymers provide advantages over micron-filled polymers because they provide resistance to degradation [1], and improvement in thermo-mechanical properties without causing a reduction in dielectric strength [2]. For example, an increase in dielectric strength and a reduction in space charge has been documented for the case of nano-TiO2 filled epoxy resin over micron size TiO2 filled epoxy composites [3]. Also, recently published results for electrical voltage endurance in these new materials indicate that very substantial (3 orders of magnitude) improvements in voltage endurance can be demonstrated. These improvements in dielectric properties observed for nano-filled polymers could be due to several factors: (i) the large surface area of nanoparticles which creates a large 'interaction zone' or region of altered polymer behavior [4], (ii) changes in the polymer morphology due to the surfaces of particles [5], (iii) a reduction in the internal field caused by the decrease in size of the particles, (iv) changes in the space charge distribution [6, 7], and (v) a scattering mechanism. It should also be recognized that this technology also results in characteristic changes in non-electrical properties that have been found beneficial as detailed in references from a recent review paper [8].

The internal surfaces are critical in determining the properties of nano-filled materials. Nanoparticles have high surface area-to-volume ratio; particularly when the size decreases below 100 nm. This high surface area-to-

Manuscript received on 7 March 2005, in final form on 31 May 2005.

volume ratio means that for the same particle loading, nanocomposites will have a much greater interfacial area than microcomposites. This interfacial area leads to a significant volume fraction of polymer surrounding the particle that is affected by the particle surface and has properties different from the bulk polymer (interaction zone) [4]. Since this interaction zone is much more extensive for nanocomposites than for microcomposites, it can have significant impact on properties [9, 10]. For example, depending upon the strength of the interaction between polymer and particle, this region can have a higher or lower mobility than the bulk material, and result in an increase [11] or decrease [2] in glass transition temperature [9]. It has also been suggested that free volume in such interaction zones is altered by the introduction of nanofillers. Since, these interaction zones are likely to overlap at relatively low volume fractions in nanocomposites, a small amount of nanofiller has been found to impact the electrical behavior [12, 13]. Some authors have emphasized that the interaction zone around the particles is a "quasi-conductive" region which partially overlaps in the nanocomposites [13]. These overlapped interface regions thus may allow charge dissipation, which, in turn, could be expected to improve the dielectric breakdown strength and voltage endurance characteristics.

Introduction of a second phase can also influence the breakdown strength of the dielectrics via a scattering mechanism [14] (i.e. an increase in path length of the carriers responsible for the breakdown processes) or, by changing the space charge distribution [15]. It has been shown by some authors that when the size of the filler approaches the chain conformation length, they act 'cooperatively' with the host structure either eliminating or suppressing Maxwell-Wagner polarization, which is well-known in the case of conventionally filled materials [3]. Some recent results also suggest that it is the size of the filler that plays the most crucial role in terms of global properties (electrical, mechanical and thermal), rather than the chemistry of the particles [16]. Finally, changes in morphology due to incorporating nanoparticles can influence the dielectric behavior of nanocomposites [17]. The large surface area can also lead to changes in the morphology of semicrystalline polymers as observed by several groups [5, 17]. The breakdown strength of the intraspherulitic regions is higher than that of the interspherulitic regions and a change in the disorder within the spherulites or of the interspherulitic region can affect the breakdown strength.

The promise of unique electrical properties due to the mechanisms just described provides an incentive for investigating the dielectric properties of nano-filled materials. In order to obtain a better understanding of the role of the nanoparticles in the process of dielectric breakdown, lifetime, and space charge behavior, the interfacial region needs to be investigated. Interfacial characteristics are not only determined by the size-induced properties, but also the surface chemistry of the particles. Therefore, in this paper both as- received and surface modified nanoscale silica was used since experience has indicated that chemical coupling can have beneficial effects [17]. Therefore, in this paper both untreated and surface modified nanoscale silica was used, and the interface was characterized using several techniques. An attempt is made to connect the behavior at the interface to the breakdown strength, and provide some insight.

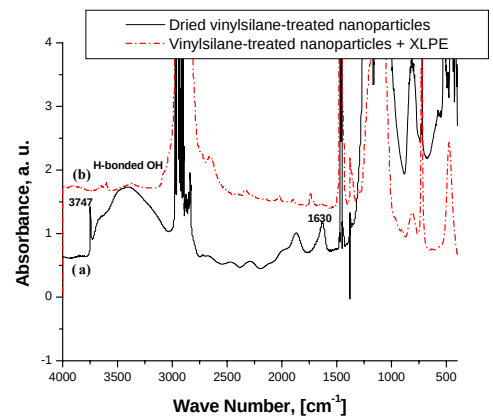

Figure 1. FTIR spectra. a, vinylsilane treated nano-silica powders; b, vinylsilane treated nanocomposite.

2 EXPERIMENTAL DETAILS

2.1 SYSTEM INVESTIGATED

The material studied here is a SiO_2-polyethylene composite which has been formulated utilizing micro and nano particulates. The base polyethylene is a commercially available material already in use in the manufacturing of high-voltage (HV) extruded cross-linked underground cables. It is a high purity, filtered resin containing antioxidants. These additives are non-ionic and do not contribute to the base polymer conductivity. The polyethylene contains the cross-linking agent dicumyl peroxide (DCP), which reacts at temperatures above the compounding temperature creating a crosslinked matrix. Some untreated nanosilica was surface-modified with triethoxyvinylsilane.

Figure 1 shows FTIR spectra of vinylsilane-treated particles and vinylsilane-treated nanofillers in XLPE indicating that the surface treatment resulted in covalent bonding between the nanoparticles and the XLPE. There are two significant differences between these spectra: (1) many of the features of the particles (such as free silanol groups at 3747 cm^{-1} and a broad peak centered around 3500 cm^{-1}) are gone, and (2) some new features are added. A peak at 1580-1680 cm^{-1} representing carbon-carbon double bond (-C=C-) which was present in the vinylsilane-treated particles (from the vinyl group) is replaced by the peak at 2860-2970 cm^{-1}

representing the single bond of carbon ($-CH_2-CH_2-$) [18]. This leads one to conclude that vinyltriethoxysilane is chemically bonded to silica particle on one end, and to polyethylene on the other. A schematic of the possible chemical reaction of the silica particle with vinylsilane treatment with the XLPE is shown in Figure 2.

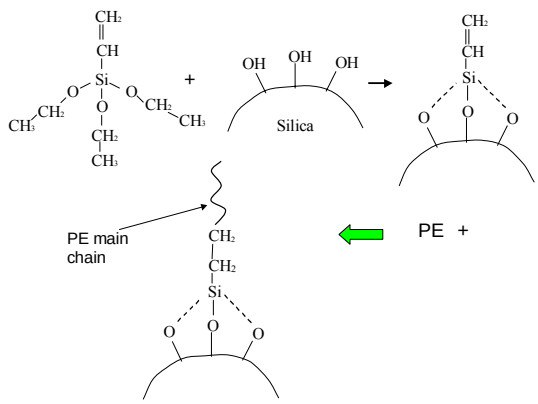

Figure 2. Summary of the chemical-route for the attachment of the vinylsilane to the surface of the nanosilica particles, and the incorporation of the modified silica into XLPE.

Proper dispersion of filler, crosslinking, and elimination of crosslinking byproducts are essential to achieving the optimum properties of the nanocomposite. Since adsorbed water will cause particle agglomeration, dynamic vacuum drying of all the micro and nano-particles was carried out at 195 ºC for 24 h immediately prior to compounding (except the vinylsilane-treated particulates which were dried at 160 ºC). The composite was mixed with a melt mixer above the melting temperature of the polymer. Figure 3 shows a SEM micrograph of a typical dispersion observed in all the nanocomposites tested.

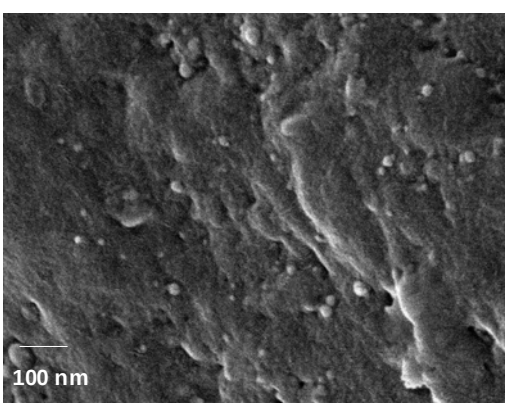

Figure 3. SEM micrograph of XLPE with 5% untreated nanosilica

Three types of samples were formulated: (i) a sample with multiple recesses was used for breakdown strength measurements, (ii) laminar samples were used for dielectric spectroscopy and pulsed electroacoustic analysis (PEA), (iii) a cylindrical block with an embedded electrolytically-etched tungsten electrode which created divergent field geometry was used for voltage endurance evaluations. All samples were created by hot pressing, and then allowed to cool slowly to room temperature, keeping the pressure constant. The samples were post-cured under vacuum. The samples meant for electrical testing were metallized to a thickness of ~150 Å by sputtering gold. Melt processing and post-cure annealing are likely to mitigate the presence of pre-existing electric charge.

2.2 THERMOMECHANICAL CHARACTERISTICS

The degree of crystallinity and melting temperature of the processed samples were measured using Differential Scanning Calorimetry (DSC). The samples were heated from room temperature (25 ºC) to 150 ºC at a rate of 10 ºC per minute. The temperature was held constant at 150 ºC for 5 minutes before the sample was cooled to room temperature at a rate of 10 ºC per minute. This cycle was repeated twice for each sample and the second peak was considered for calculation [19]. The weight of the sample for each experiment was approximately 5 mg. A set of four specimens was used for each type of formulation, and the right tangential method was used to determine the crystallinity of the samples. Table 1 summarizes the DSC tests. Table 1 shows that the degree of crystallinity of micro- and untreated nanocomposites are in a similar range whereas the vinylsilane-treated nanocomposite has ~ 33% higher crystallinity than the other composites.

Table 1. Crystallinity and melting point data for XLPE materials from DSC measurements.

Sample Type	Degree of crystallinity (%)	Melting Point (ºC)
XLPE Only	45 ± 1	103.2 ± 1.4
5% untreated nanosilica + XLPE	44 ± 1	109.0 ± 0.5
5% vinylsilane treated nanosilica + XLPE	60 ± 1	108.1 ± 1.1
5% untreated microsilica + XLPE	44 ± 1	108.3 ± 1.2

Changes in glass transition temperature can indicate altered polymer chain mobility. Glass transition temperature was measured using a Rheometric Scientific DMTA (Model-V). Glass transition temperature measured from a mechanical loss peak and mechanical loss factor [20] shows that the glass transition temperature for nanocomposites is ~ 5 ºC higher than base resin.

2.3 ELECTRICAL CHARACTERIZATION

2.3.1. PRACTICAL MEASUREMENTS

Dielectric breakdown strength, space charge

determinations, voltage endurance measurements, and dielectric spectroscopy were conducted for the base polymer and composites.

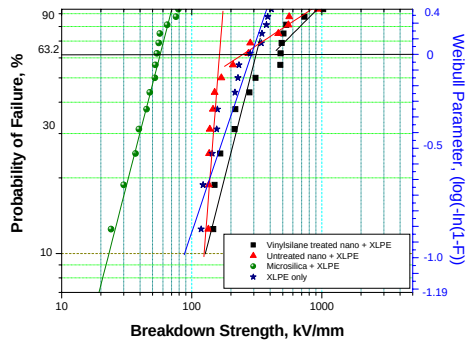

Figure 4. Weibull plot for the dielectric breakdown strength of XLPE with 5 weight percentage micro- and untreated and vinylsilane-treated nano-silica measured at 25ºC.

2.3.2 DIELECTRIC BREAKDOWN STRENGTH MEASUREMENTS

The breakdown strength of the micro- and nano-composites were compared to the base resin. Multiple recessed specimens with gold electrodes were used for the measurements. A conventional 2-parameter Weibull distribution was used to analyze the breakdown data for samples ranging in thickness from 0.15 mm to 0.015 mm (Figure 4). This distribution has been found to be the most appropriate for electrical strength analysis and is described in detail elsewhere [21, 22]. The cumulative probability P of the electrical failure takes the form of:

$$P = 1 - \exp\left[-\left(\frac{E}{E_0}\right)\right]^{\beta} \qquad (1)$$

where β is a shape parameter and E_0 is a scale parameter that represents the breakdown strength at the cumulative failure probability of 63.2%. Breakdown tests were conducted at four different temperatures (25, 60, 70 and 80 ºC) to study the effect of temperature on the breakdown phenomenon.

2.3.3 SPACE CHARGE MEASUREMENTS

Pulsed electro-acoustic tests were conducted (courtesy of the University of Leicester, UK) to assess the field distortion in the bulk samples. Laminar samples of approximately 0.5 mm thickness, with sputter deposited gold electrodes on both sides were utilized for these tests. Space charge was measured periodically during the charging and discharging periods. All the tests were conducted at room temperature (293±3 K).

2.3.4 VOLTAGE ENDURANCE MEASUREMENTS

Voltage endurance characteristics of both the base polymer and nanocomposites were measured by subjecting the samples to long-term endurance tests. The samples were cylindrical blocks of polymer or polymer nanocomposite, embedded with a tungsten electrode of tip radius, r, of approximately 4 µm (for more divergent field) and 12 µm (for less divergent field), with an inter-electrode distance, d, of ~2 mm. The samples were stressed with a 60 Hz alternating voltage, and the applied voltage, V, is translated into calculated tip stress, E, using the relationship [3]:

$$E = \frac{2V}{r\ln(4d/r)} \qquad (2)$$

2.3.5 DIELECTRIC SPECTROSCOPY MEASUREMENTS

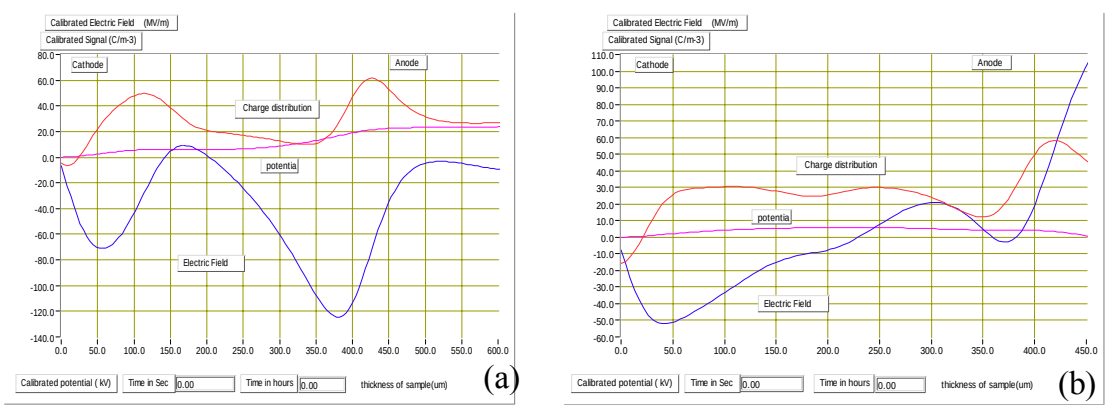

Figure 5. Typical PEA space charge measurements. a, XLPE only; b, nano-filled material.

Dielectric spectroscopic measurements were undertaken for base polymer, micro-filled, nano-filled, and surface modified nano-filled composites at various temperatures using a Novocontrol Alpha Analyzer (type K) in combination with a Novocontrol active BDS-1200 sample cell. Laminar samples of thickness approximately 0.5 mm with gold electrode sputtered into a circular area of 2.2 cm were used for dielectric spectroscopy measurements.

3 RESULTS

3.1 RESULTS OBTAINED FROM ELECTRICAL CHARACTERIZATION

The characteristic breakdown strength for XLPE at room temperature is found to be 269 kV/mm, which is comparable to published values [23]. There is a dramatic increase in breakdown strength for the untreated nanofilled composites over the micron-filled counterparts shown in Figure 4. However, the largest increase was observed for the vinylsilane treated silica/XLPE composite. In addition, the vinylsilane treated silica/XLPE samples maintained their breakdown strength at elevated temperature (decreasing by a factor of 2 only at 80 ºC). For all other samples, the strength decreased by a factor of about 3 as the temperature was increased to 80 ºC. However, the Weibull shape parameter (β) increases for all the samples at 80ºC temperature indicating a smaller spread in the breakdown voltage. This decrease in breakdown strength is expected as there is an increase in free volume with temperature [24].

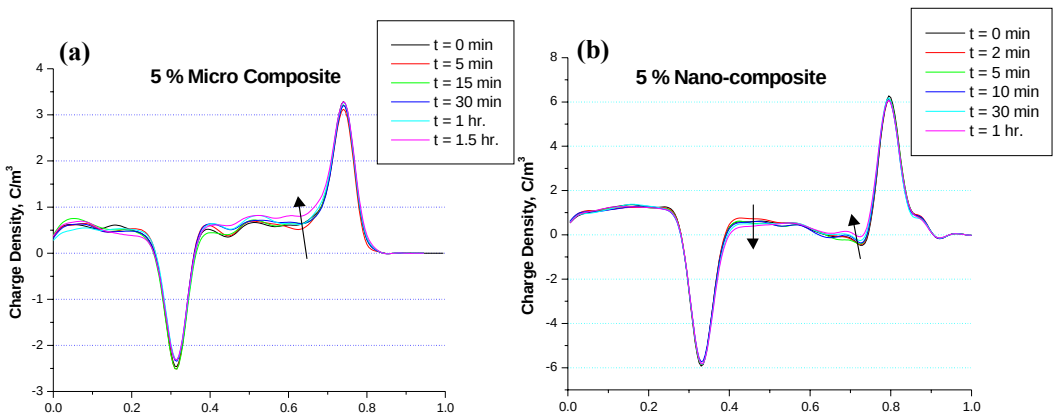

Figure 6. Charge dynamics in **(a)** micro-filled material, **(b)** nano-filled material, during charging of the samples. The arrows show the charge development over time (2 min to 1 h).

Figures 5(a) and 5(b) show typical PEA measurements of the base resin (XLPE) and 10% nanosilica loaded composite after one hour of stressing at 6 kV_{dc}. The curves show the distribution of charge density, electric field and potential between the electrodes. It can be seen that the charge levels in the nano-filled composite are reduced in comparison with

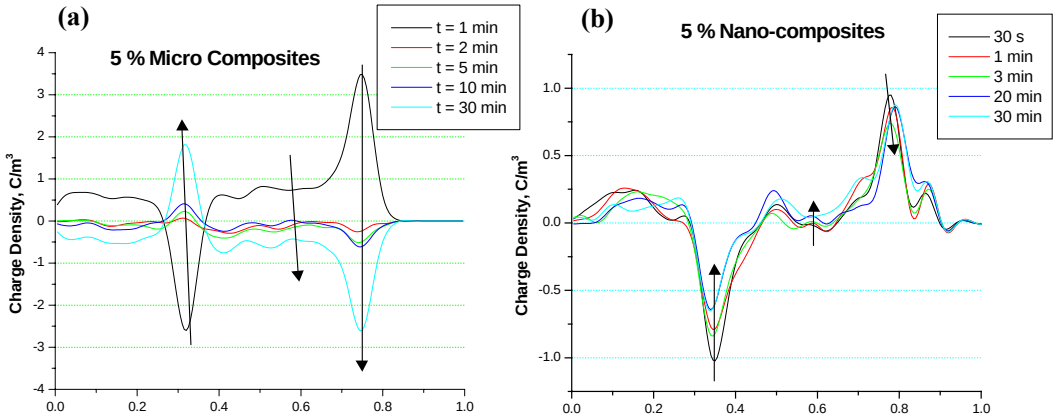

Figure 7. Charge dynamics in **(a)** micro-filled material, **(b)** nano-filled material, during discharging of the samples. The arrows show the charge development over time (1 min to 30 min).

the base polymer (note the change of scale). Also, the charge distribution of the nano-filled composite is more uniform than in the base polymer.

Figures 6(a) and 6(b) show the charge distribution dynamics for the micro- and nano-filled materials during the charging process. There are some differences in charge build-up pattern between micro and nano-filled materials. For the nano-filled material, there is a heterocharge build-up near both the electrodes, whereas in the case of micro-filled material heterocharge builds-up near the cathode and homocharge near the anode. The charge build-up within the bulk is at lower levels for the nano-material (~ 50 %). Since, local charges may move more easily in nano-filled material than in micro-filled material, electrode charges decrease over time. For micro-filled material more positive charge is injected over time, which might be the reason for an increase of the bulk charge and broadening of the anodic peak.

decreases with time. However, for micro-filled material this is completely different. Up to one minute the pattern is similar to the build-up pattern, thereafter the polarity of the electrode is reversed indicating an accumulation of opposite charge. This behavior is very different from the behavior of micro-filled composites of other systems (e.g. titania and epoxy) as discussed by various authors [3, 6].

The superior performance of nanofilled material over base resin is best demonstrated by a voltage endurance test. For tip stresses above 500 kV/mm, the XLPE breaks down almost immediately (within a matter of two hours, which is reduced to less than an hour at 600 kV/mm). In contrast, the filled materials exhibit a time to failure which is **two and half orders of magnitude higher** than the base resin. It is clear that the less divergent (more uniform) field specimens (represented as open symbols in Figure 8) and the more divergent field

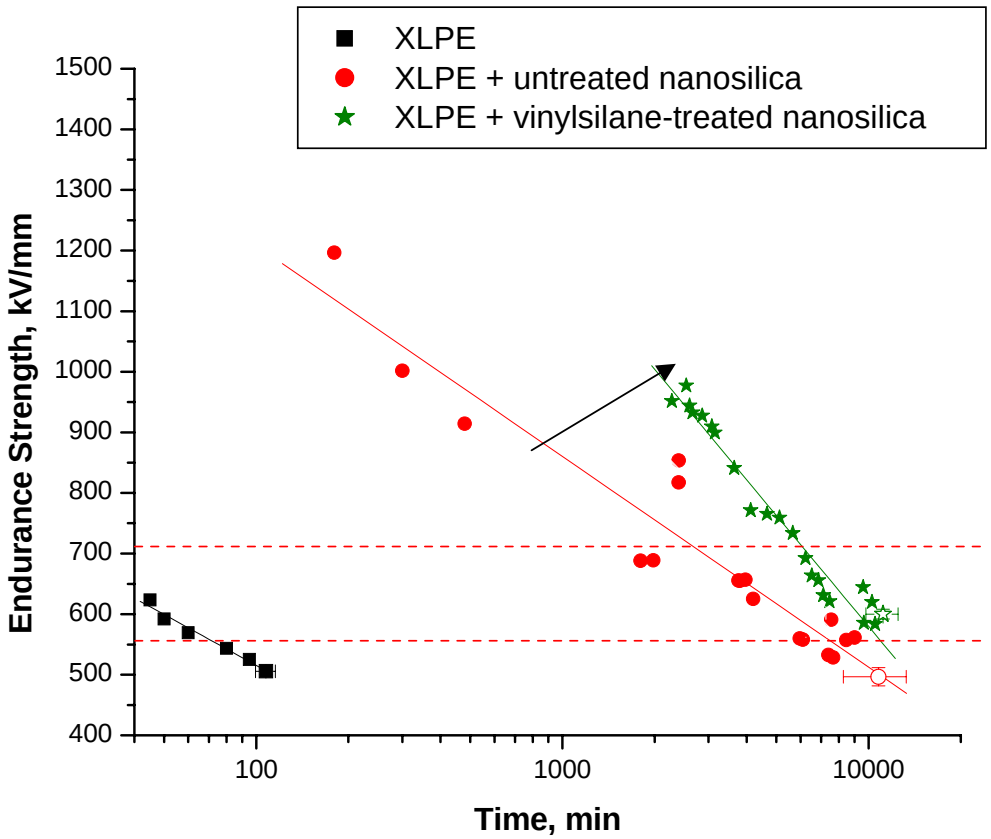

Figure 8. Voltage endurance of XLPE based composites using divergent (filled symbols) and less divergent (open symbols) fields, compared with the base resin.

Figures 7(a) and 7(b) show the corresponding charge dynamics for the micro- and nano-filled materials during the discharging process. For nano-filled material the discharge pattern gradually

specimens lead to similar endurance times at lower tip stress. This suggests that as soon as a channel is initiated it propagates to failure. The highest endurance time is

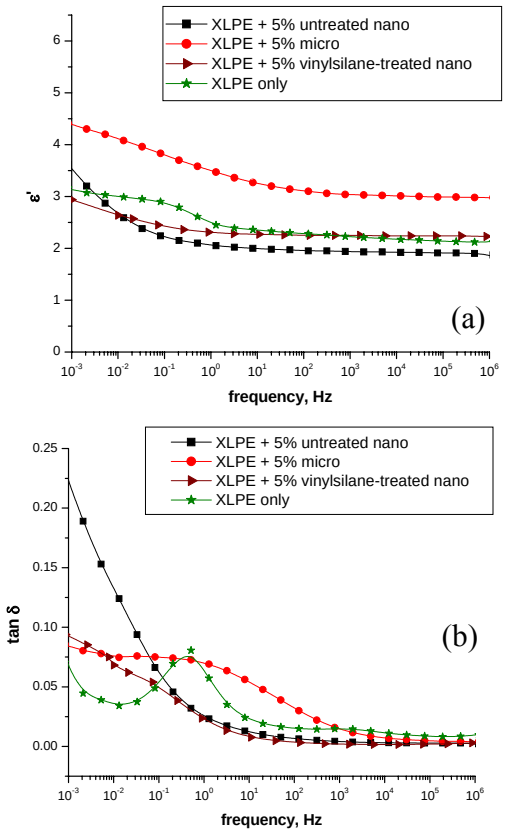

Figure 9. Real part of permittivity **(a)** and loss tangent **(b)** for micro filled materials, untreated and surface-treated nanofilled materials and base resin versus frequency. All loadings are 5 wt%.

shown by the vinylsilane-treated nanosilica filler material, with twice the time to failure as compared to untreated nanosilica filled materials for similar stress levels. However, Figure 8 suggests that the voltage endurance curve slopes of functionalized and non-functionalized nanocomposites are different. This implies that the treated material is more effective at the higher stress levels where the improved bonding plays a greater role.

Figures 9(a) and 9(b) show the change in permittivity and tan δ as a function of frequency at 25 ºC for the base resin as well as the micron filled and nanofilled XLPE. The responses in Figure 9a, comparing micro and nano-filled materials for similar loading levels are alike, although the micro-filled material shows a significant increase in permittivity throughout the frequency range investigated. The untreated composite permittivity at power frequencies when calculated using the Lichtenecker-Rother logarithmic formula [25], Maxwell-Garnet random mixing formula [26], and Landau-Lifshitz power law formula [27], with a power factor (exponential term in power law equation) of 1/3, yields approximately 2.23 (at 60 Hz) in all cases, a little higher than the base resin. However, this is lower than the measured value of 3.14 for 5% micro-filled material, suggesting that some interfacial polarization is present. However, there is a decrease in permittivity for the nanocomposite to a level lower than the base resin (for PE it is ≈ 2.2) with

Table 2. Calculated low frequency activation energies for silica composites.

Sample Name	Activation Energy (eV)
XLPE + 5% untreated nanosilica	0.18 ± 0.05
XLPE + 5% vinylsilane-treated nanosilica	0.18 ± 0.09
XLPE + 5% microsilica	0.28 ± 0.06

incorporation of 5% nanofiller. This is true at all temperatures (not shown in the figure). Figure 9(b) compares the loss tangent of micro- and nano-filled materials. The broad loss peak, which appears in micro-filled materials, is completely eliminated for the nano-filled materials. The nanoparticles appear to reduce the chain movement of the polymer through physical bonding or through confinement. The 5 °C increase in glass transition temperature documented in Section 2.2 may provide support for this. This is also consistent with improvement of the breakdown strength of the nanocomposites, where the physical bonding between nanoparticles and the polymer chain could be responsible for the increase in breakdown strength. There is a decrease in permittivity with increase in temperature for both sizes of filler. This is expected, as there is a decrease in dielectric constant of the filler itself with increasing temperature [28, 29], and also an increase in the amount of free volume with temperature [24]. Also, the Maxwell-Wagner effect is either not produced or suppressed as evidenced by the permittivity remaining constant over a considerable frequency range [30]. In the case of nanosilica filled materials, the permittivity is unchanged for a given temperature for a wide range of frequency (0.1 Hz – 1 MHz), but starts to increase due to 'quasi-dc' conduction [31] at lower frequencies. This 'quasi-dc' conduction has been explained by Lewis [32] utilizing the O'Konski's model [33] and a double layer approach. By this model, charge carriers are efficiently transferred around the interface by the field leading to an induced polarization at the polar ends of the particle which becomes a large dipole [32]. This will lead to a dielectric constant higher than the particle itself. Since these double layer effects are likely to be pronounced in nanocomposites, the slope of the permittivity is steeper than for the microcomposite in the low frequency region.

The real part of the permittivity (Figure 9(a)) of the vinylsilane-treated nanosilica composite is comparable to the untreated nanosilica and the unfilled XLPE at high frequency. At low frequency, both nanocomposites show a lower permittivity. On the other hand, the tan δ behavior of

the vinylsilane treated nanosilica is different from the untreated nanofilled composite (Figure 9(b)). The slope of the 'quasi-dc' part is lower than the untreated nanofilled composite, suggesting that the conducting sheath present in the case of untreated nanofilled material is less-conducting here.

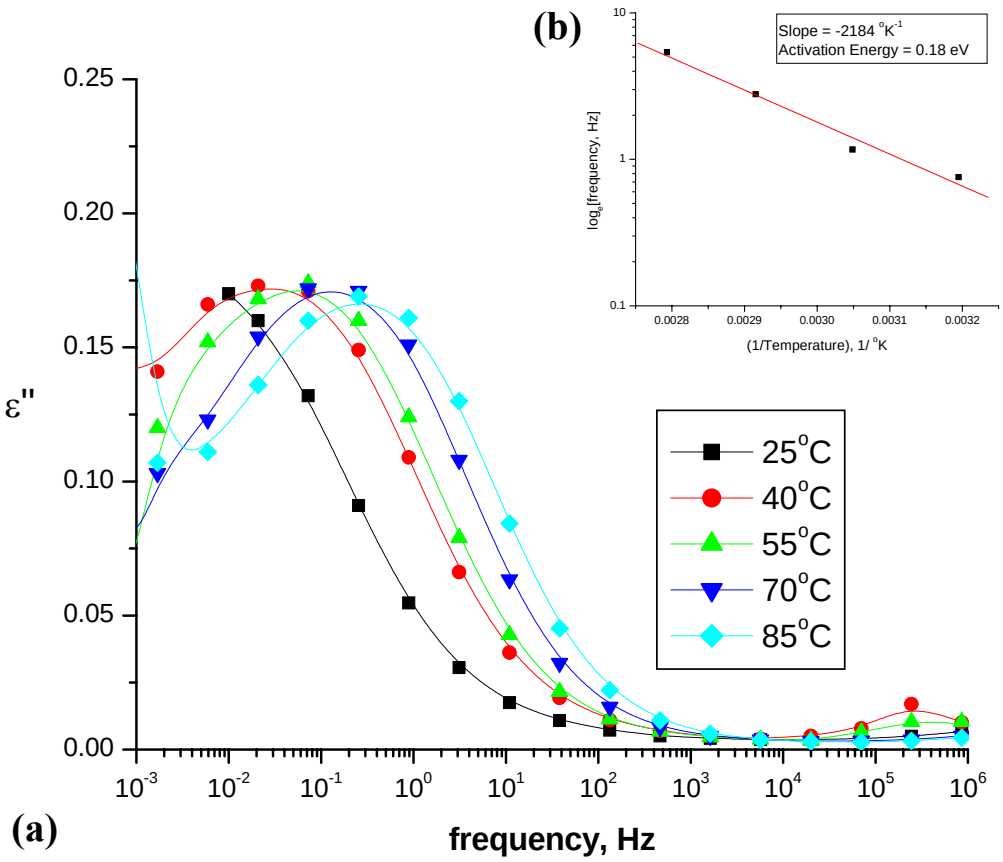

Figure 10. a, Imaginary relative permittivity of a typical vinylsilane treated nanosilica composite versus frequency at measured temperatures; b, activation energy of low frequency processes presented in (a).

Figures 10(a) and 10(b) show a typical temperature dependence of the imaginary relative permittivity as a function of frequency and an Arrhenius plot for low frequency processes for the vinylsilane treated nanosilica composite. The activation energy (shown in Figure 10b was calculated by the normalization method [34] by shifting the frequency spectra laterally and then determining the frequency shift required to bring the curves into coincidence. Similar measurements were also made for other nano and micro composites and the activation energy for each are given in Table 2. Table 2 suggests that highest breakdown strength material, the vinylsilane treated nanosilica composite, has an activation energy similar to untreated nanosilica composites and hence similar polymer interfacial mobility as suggested by a similarity in the imaginary parts of the permittivity for vinylsilane-treated and untreated nanosilica composites.

3.2 CHEMICAL CHARACTERIZATION

3.2.1 CHARACTERIZATION USING FOURIER TRANSFORMED INFRA-RED (FTIR)

A Nicolet NEXUS 470-ESP FTIR spectrometer was employed to take the spectra of both the particles themselves and the associated composites samples. To investigate the nature of the particles before incorporation into a composite, the particles were compressed into pellets approximately 0.8 mm in thickness, and, for composite measurements, laminar samples of approximately 1 mm thickness were used.

Figure 11 shows the FTIR spectra for (a) the nanoparticles and (b) the microparticles. The sharp band at 3747 cm^{-1}, present only in nanoparticles, is attributed to isolated silanols and the broad absorption band around 3500 cm^{-1} (more pronounced in the microparticle sample) has been assigned to the (OH) stretching vibration of surface hydroxyl groups involved in hydrogen bonds with water molecules and with adjacent silanol groups [35]. The band at 1630 cm^{-1} corresponding to the (OH) bending vibration of adsorbed water molecules, decreased for nanoparticles. Based on the above results, changes in the surface silanol structure for

particles of two different sizes can be illustrated in Figure 12. For relatively large particles, most of the silanol groups are hydrogen-bonded to each other and this imparts some polarity to those silanol groups (Figure 12(a)). For particles of nanoscale diameter, the high surface curvature increases the distance between the silanol groups preventing hydrogen bonding between them (Figure 12(b)). [36].

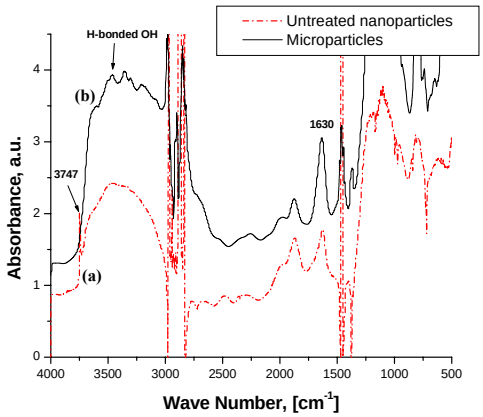

Figure 11. FTIR surface spectra of silica powders. a, nanometric size; b, micrometer size.

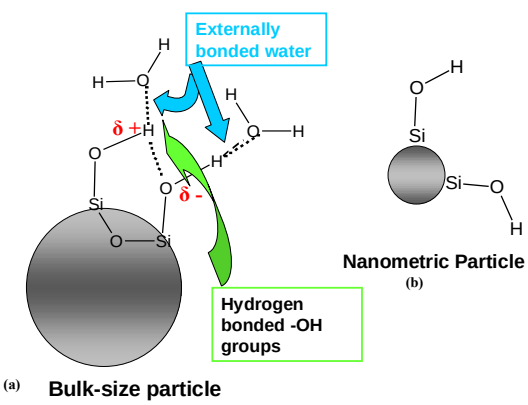

Figure 12. Schematic of two different sizes of particles, a, micrometer size; b, nanometric size. Bulk-size particles have hydrogen bonding between the nearest O and H of the silanol groups; this is absent in nanometric size particles.

3.2.2 CHARACTERIZATION USING ELECTRON PARAMAGNETIC RESONANCE (EPR)

The Electron Paramagnetic Resonance (EPR) spectra show evidence of changes in the interface chemistry due to composite processing. The microwave magnetic field component perpendicular to the direction of the field causes EPR transitions when the microwave quantum energy, $h\upsilon$ (where υ is the frequency and h is Plank's constant), is equal to the Zeeman energy splitting $g\beta H$ of two energy states (M = ½ and M = - ½),

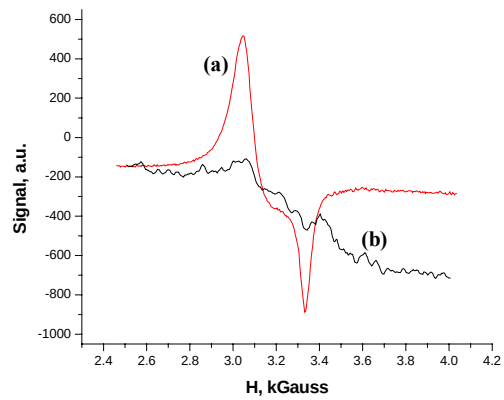

Figure 13. EPR spectra of **(a)** nanosilica and **(b)** microsilica.

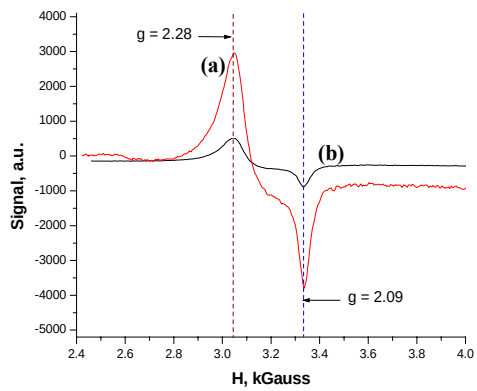

Figure 14. EPR spectra of **(a)** nanocomposite and **(b)** nanosilica powder (same as Figure 13 (a)).

i.e. $h\upsilon = g\beta H$. The parameter g (called Lande's g factor) is the spectroscopic splitting factor representing the nature of the unpaired electron and β is the unit of magnetic moment called the Bohr magneton [37, 38]. Each type of unpaired electron is identified with the appropriate g factor obtained from the resonance condition as $g = (h/\beta)(\upsilon/H)$. All the powdered silica samples and composites (cryo-crushed) were measured using a Bruker ER 042 EPR spectrometer. The g value calibration was done before and after the measurement using dpph, which has g value of 2.0039 (the g value for a free electron is 2.0023). All the curves presented for the analysis are the derivative of microwave absorption at 9.77 GHz plotted as a function of the applied magnetic field and are normalized for comparison. In the case of powder samples containing anisotropic defects, as is the case here, the spectra become quite complicated in appearance.

Figure 13 shows the EPR spectra for micro and nanosilica powders dried at 195 ºC. The peak shown by nanoparticles (Figure 13(a)) is "well defined", whereas in the spectra for

micro particles (Figure 13(b)), the species responsible for the peak is broader and not "well defined", and of lower intensity. The term "well defined" here implies that, in the case of nanoparticles, most of the radical centers have the same crystallographic environment. For the microparticles, however, the environments of the radicals are more diverse. The positions of upper and lower bound extrema, at g values of 2.28 and 2.09 respectively, strongly suggest that the responsible species for the spectra are diatomic oxygen (O^-_2). The surface treated nanoparticles have an EPR signature similar to microparticles. The magnitude of the spectra, which are proportional to the number of radicals, increases when the particles are incorporated into the polymer (Figure 14). This is true for all particles. Table 3 shows the peak signal height of particles alone and of the 5% loaded composite. The signal is normalized with respect to power and sensitivity of equipment, but not to the volume fraction of particles (composites have 5 wt% of particles). Although the resurgence of oxygen radicals is lower for surface-treated nanosilica fillers compared with untreated nanosilica fillers, the trend of increasing oxygen radicals is evident.

Table 3. Peak EPR signal for powdered samples and 5 wt% composites.

Material	Signal (a.u.)	
	Powder	Composites
Micro	550	1600
Untreated nano	6000	6600
Vinylsilane treated nano	550	1300

3.2.3 CHARACTERIZATIONS USING X-RAY PHOTOELECTRON SPECTROSCOPY (XPS)

X-ray Photoelectron Spectroscopy (XPS) was utilized to investigate the surface chemistry characteristics for all nanoparticles and microparticles. XPS analysis was done on a Perkin Elmer (Model # 5500) using Mg K_α monochromatic radiation. Data was gathered before argon cleaning and after 3 min, 6 min and 9 min of argon cleaning; it was found that the data was similar in peak position and intensity. Data gathered were analyzed using Auger Scan-2 software which employs a linear least squares optimization with a simplex peak fitting algorithm. The background was displayed in the curve fit.

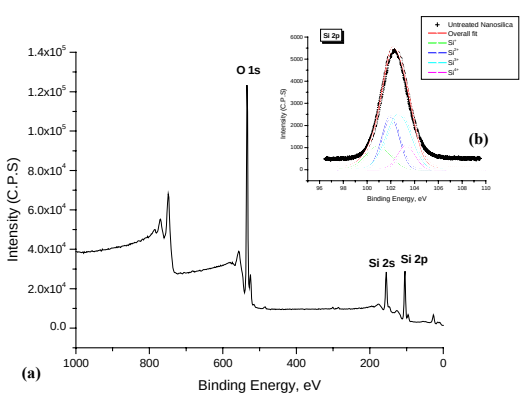

Figure 15. **(a)** Survey XPS spectrum of untreated nanosilica after 3 min of Ar cleaning showing oxygen and silicon peak **(b)** deconvolution of Si 2p peak.

XPS analysis indicates that the surface of the particle contains mainly oxygen and silicon for the untreated particles (Figure 15) and traces of carbon and nitrogen, in addition, for the surface treated particles. To discern the small differences in peak position due to different chemical states of silicon, curve fitting was performed using peak positions taken from the literature [39, 40]. These four chemical structures (Si^+, Si^{2+}, Si^{3+} and Si^{4+}) and the corresponding Si 2p binding energies are given in Table 4. Each component is fitted with symmetrical Gaussian fit. In each fit the alternative peak positions were kept at the same width while the intensity was adjusted. From the intensity of the peaks the stoichiometric formula SiO_x was calculated using the formula:

$$x = \left[\frac{\sum_{i=1}^{4} n_i H_i}{\sum_{i=1}^{4} H_i} \right] \qquad (3)$$

where n is the oxidation state of silicon and H is the peak intensity.

Table 4. Silicon chemical environments and corresponding binding energies [38, 39].

Structure	R | R—Si—O | R	O | R—Si—O | R	O | R—Si—O | O	O | O—Si—O | O
Abbreviation	$Si(-O)_1$	$Si(-O)_2$	$Si(-O)_3$	$Si(-O)_4$
Binding Energy (eV)	101.8	102.1	102.8	103.4

3.2.4 THE EMERGING PICTURE OF THE INTERFACE

The XPS data suggests that the oxygen content in the vinylsilane treated silica is lower than in the untreated nano- and microsilica. The EPR data supports this. The lower oxygen content may be explained with the help of Figure 2, which shows the surface chemistry for the silica particle when it is treated with vinylsilane. Silicon from vinylsilane chemically bonds to oxygen, which possibly originates from either surface silanol or oxygen radicals (O^-), which are present on the surface [41]. The reaction will favor oxygen radicals because oxygen radicals have higher energy. Therefore, the low oxygen content is because of the vinylsilane reaction. This leads to numerous Si-Si bonds in the particle and those can be treated as oxygen defects on the surface of the particle [42]. These oxygen defects act as the trap sites for charge carriers which might explain the increase in breakdown strength. In addition, the surface treated groups can affect the dielectric properties in several ways. The

vinylsilane chemically bonds to the surface of the nanoparticle and the polymeric chain thereby reducing the de-wetting of the filler surface. These radially extended silane moieties can redistribute the counter ions by changing their screening length and distribution pattern due to the introduction of electrophilic elements present in the modifier groups (silicon here) [43].

4 DISCUSSION AND APPRAISAL

The introduction of a large interaction zone with reduced mobility (increase in T_g) imparts a significant change to the electrical properties. Therefore, understanding the electrical behavior necessitates knowledge of the underlying physics and chemistry of the interaction zone. This will clearly require much more characterization of these materials if specific new mechanisms of a mesoscopic mature originating from the nano interfaces (e.g. new trapping phenomena) are to be undercovered.

Breakdown of polymeric dielectrics is affected by several factors, such as degree of crystallinity [44], accumulation of bulk charge [3, 6], interfacial area [17], type of bonding, temperature, and free volume [45-47]. There is no significant difference in crystallinity among the composites except for the sample where the fillers are treated with vinylsilane, which resulted in a 33% increase in crystallinity. The vinylsilane-treated nanoparticles did result in the composite with the highest breakdown strength; but, the largest increase in breakdown strength was for nanoparticles as compared to micron particles where no significant change in crystallinity occurred. Hence, crystallinity does not appear to be a dominant factor here in determining electric strength.

The finding that micron filled materials are accompanied by a higher bulk charge accumulation than the nanofilled material points to a reason for the lower electric strength of micron filled materials. Lowering of the bulk charge in nanofilled material, even in comparison to the base polymer, provides a basis for engineering a material to exhibit an electric strength commensurate with the base polymer. It has been postulated that nanoparticles reduce the bulk charge accumulation by introducing a local conducting path through the overlapping of nanometric double layers [32]. This can occur for nanocomposites at lower loadings, unlike microcomposites where the volume fraction of the dielectric double layer is still very low. This results from the 3 orders of magnitude increase in surface area for the same wt% loading. The marked low frequency loss depicted in Figure 7(b) for the untreated nanocomposite is noticeably absent for the case where a vinylsilane surface treatment has been applied. The charging of the silica particles while performing the XPS study suggests that the surface of the vinylsilane treated nanosilica per se is insulating in nature. In vinylsilane-treated nanocomposites the chains are covalently attached to the nanoparticles, most likely increasing interfacial polymer density and reducing the micro-defects in the interface. These changes in local density of polymer are under investigation.

The reduction in dielectric strength of polymeric materials with increasing temperature is attributed to the existing free volume in the polymer [44]. In the free volume approach, pioneered by Artbauer [47], attempts were made to relate electronic breakdown strength to the acceleration of charge carriers, which is essentially related to free volume. These parameters can be related as follows:

$$E_b = \frac{W_{th}}{el_x} \tag{4}$$

where W_{th} is the energy needed to break the bond of the polymeric chain, E_b is the applied electric field, e is the charge of the electron, and l_x is the mean distance traveled by the electron before it encounters a collision. The calculation for l_x using Equation 4, assuming a carbon-carbon (-C-C-) bond strength of 3.8 eV [48] and an applied field of 1 MV/mm, suggests that l_x is ~40 nm, which is an order magnitude higher than the typical free volume lengths at room temperature for most polymers [49, 50]. This implies that the small increase in free volume between 25 to 60ºC does not significantly affect the breakdown strength of the composites. For LDPE, l_x is ~5 nm between T_g and the melting point; above the melting point lx drastically increases to about 20 nm, reducing the breakdown strength significantly [51]. The melting of the crystalline parts of XLPE starts at about 75 ºC, as evidenced by the endothermic part of a DSC plot. Hence the breakdown strength decreases sharply above that temperature, owing to the drastic increase in free volume [52]. Also, for LDPE there exists a good correlation between the breakdown strength and cohesive energy density [45], which is a measure of the binding forces between molecular chains of the polymer. This dependence of breakdown strength on cohesive energy density and free volume suggests that the breakdown mechanism involves some structural deformation and polymeric chain scission [51].

A dramatic improvement in electrical properties of nanofilled material over base resin is demonstrated in the voltage endurance tests depicted in Figure 8. An improvement of two and half orders of magnitude in lifetime for untreated nanofilled material over base resin clearly provides an opportunity for the design of new materials. A cavity formation and propagation mechanism can be utilized for a possible explanation. It can be concluded by comparing the divergent specimens with less divergent specimens that, it is the crack initiation time that improves the life of the filled specimens, but, once the cracks are beyond a threshold limit, they propagate rapidly causing the failure of the samples. This crack threshold size limit may be different for different types of bonding. Also, among the nano-filled materials, untreated filled materials have shorter lifetimes than chemically bonded filler materials such as the vinylsilane-treated nanofilled polyethylene. At higher and divergent fields, surface-treated filled materials perform better then untreated ones, as indicated by the increase in slope of the line corresponding to surface-treated nanofilled materials. The improvement of lifetime for surface treated

filled materials could be attributed to the formation of chemical bonds, which reduces the chances of particle surface de-wetting and formation of the interfacial defects such as microvoids. Since the interaction zones act as transducers [32], application of electric stress produces mechanical stress. Presence or absence of these defects in the interaction zone is crucial in determining the overall failure of the composite.

The reduction in the dielectric permittivity when the nanoparticles are incorporated into base resin may be due to one, or a combination of the mechanisms described below. Dielectric spectroscopy and PEA suggest that there is a significant interfacial polarization associated with the material loaded with micron size filler, which is mitigated when the particulate size approaches the order of nanometric range. Increase in glass transition temperature of nanocomposites over base resin might suggest that there is a reduction in polymer chain mobility in the interaction zone. This reduction in chain mobility (in addition to the physical and chemical bonding of the polymer chain with silica particles, as in the case of surface treated fillers) might contribute to the reduction in polymer chain relaxation. Some recent observations of visco-elastic behavior of the nano-filled materials [53] suggest that particulates of nanometric dimensions contribute to the process of tether chain entanglement, which might have significant impact on this interaction zone. Since with nanoparticles, surface area increases, tethered zones will also become more significant and restrict the polymeric chain movement; thus lowering the permittivity.

5 CONCLUSIONS

While the evidence presented is very mixed, it would appear that the anomalous, and sometimes advantageous, properties which are emerging for nanocomposites have their origins in the behavior of the interfacial interaction zone surrounding the particulates. In this regard two main features would appear to be dominant:

- the mobility ascribed to the physical and chemical bonding occurring at the interface, and
- the formation of a double layer in the interfacial region which can influence local conductivity.

The impact of both of these mechanisms relies on the substantial increase in the interface area which is characteristic of nanocomposites. It is likely that the dominant mechanism will be very dependent on the chemistry of the components involved. This will provide a varied spectrum of properties, but, by the same token, a substantial opportunity to tailor these emerging materials to a wide variety of applications.

Based on the findings, some other preliminary conclusions can be drawn, although they must be restricted to the SiO_2-polyethylene nanomaterial:

1. The degree of crystallinity is not a predominant factor in deciding the higher breakdown strength of these nanocomposites.
2. Covalent bonding between the nanoparticles and the matrix (vinylsilane treated nanoparticles) increases the temperature at which the breakdown strength decreases.
3. The increase in interfacial region in nanocomposites creates a zone of altered polymer properties which reduces the dielectric permittivity of nanocomposites.
4. The highest voltage endurance occurs for composites with strong covalent bonding between the matrix and the filler.

6 ACKNOWLEDGEMENTS

The authors are indebted to the Electric Power Research Institute for the support of this work and to Professor J. Fothergill and Ms. Yujie Hu for assistance with some of the characterization work reported.

REFERENCES

1. M. Kozako, R. Kido, N. Fuse, Y. Ohki, T. Okamoto, and T. Tanaka, "Difference in Surface Degradation due to Partial Discharges between Polyamide Nanocomposite and Microcomposite", IEEE Conf. Electr. Insul. Dielectr. Phenomena, pp. 398-401, 2004.
2. B. J. Ash, L. S. Schadler, R. W. Siegel, T. Apple, B. C. Benicewicz, D. F. Roger, and C. J. Wiegand, "Mechanical Properties of Al_2O_3 / Polymethylmethacrylate Nanocomposites", Polymer Composites, Vol. 23, pp. 1014-25, 2002.
3. J. K. Nelson and J. C. Fothergill, "Internal Charge Behavior in Nanocomposites"; Nanotechnology, Vol. 15, pp. 586-595, 2004.
4. B. J. Ash, R. W. Siegel, and L. S. Schadler, "Glass Transition Temperature Behavior of Alumina/PMMA Nanocomposites", J. Polymer Sci. B, Vol. 42, pp. 4371-83, 2004.
5. D. Ma, Y. A. Akpalu, Y. Li, R. W. Siegel, and L. S. Schadler, "Effect of titania nanoparticles on the morphology of low density polyethylene", J. Polymer Sci. Part B, Polymer Phys., Vol. 43, pp. 463-533, 2005.
6. J. K. Nelson, J. C. Fothergill, L. A. Dissado, and W. Peasgood, "Towards an understanding of nanometric dielectrics", IEEE Conf. Electr. Insul. Dielectr. Phenomena, Mexico, pp. 295-298, 2002.
7. G. C. Montanari, D. Fabiani, F. Palmieri, D. Kaempfer, R. Thomann, and R. Mulhaupt, "Modification of Electrical Properties and Performance of EVA and PP Insulation through Nanostructure by Organophilic Silicates", IEEE Trans. Dielectr. Electr. Insul., Vol. 11, pp. 754-762, 2004.
8. M. F. Fréchette, "Reflecting on material trends: the case for nanodielectrics", Proc. 35th Sympos. electrical and

electronics insulating materials and applications in systems, Tokyo, Japan, pp 25-32, 2004.

9. M. F. Fréchette, M. Trudeau, H. D. Alamdari, and S. Boily, "Introductory remarks on Nano Dielectrics", IEEE Conf. Electr. Insul. Dielectr. Phenomena, pp. 92-99, 2001.
10. W. Peukert, H-C. Schwarzer, M. Götzinger, L. Günther, and F. Stenger, "Control of particle interfaces—the critical issue in nanoparticle technology", Adv. Powder Tech., Vol. 14, No. 4, pp. 411-426, 2003.
11. P. Cousin and P. Smith, "Dynamic mechanical properties of sulfonated polystyrene/alumina composites", J. Poly. Sc., Vol. 32, pp. 459-468, 1994.
12. T. Tanaka, G. C. Montanari, and R. Mülhaupt, "Polymer Nanocomposites as Dielectrics and Electrical Insulation-perspectives for Processing Technologies, Material Characterization and Future Applications", IEEE Trans. Dielectr. Electr. Insul., Vol. 11, pp. 763-783, 2004.
13. T. J. Lewis, "Nanometric Dielectrics", IEEE Trans. Dielectr. Electr. Insul., Vol.1, pp. 812-25, 1994.
14. F. Fujita, M. Ruike, and M. Baba, "Treeing breakdown voltage and TSC of alumina filled epoxy resin", IEEE Intern. Sympos. Electr. Insul., San Francisco, Vol. 2, pp. 738-741, 1996.
15. M. S. Khalil, P. O. Henk, and M. Henriksen, "The influence of titanium dioxide additive on the short-term DC breakdown strength of polyethylene", IEEE Intern. Sympos. Electr. Insul., Montreal, Canada, pp. 268-271, 1990.
16. J. K. Nelson, J. C. Fothergill, and M. Fu, "Dielectric Properties of Epoxy Nanocomposites containing TiO2, Al_2O_3 and ZnO fillers"; IEEE Conf. Electr. Insul. Dielectr. Phenom., pp. 406-409, 2004.
17. D. Ma, R. W. Siegel, J-I. Hong, L. S. Schadler, E. Mårtensson, and C. Önneby, "Influence of nanoparticle surfaces on the electrical breakdown strength of nanoparticle-filled low-density polyethylene", J. Mater. Res.; Vol. 19, No. 3, pp 857-72, 2003.
18. H. A. Szymanski, *Theory and Practice of Infrared Spectroscopy*, Plenum Press, New York, 1963.
19. J. R. Saffell, "Analysis of DSC Thermal Curves for Assigning a Characteristic Glass Transition Temperature, Dependent on Either the type or Thermal History of the Polymer", *Assignment of the Glass Transition*, ASTM STP 1249, Ed. American Society for Testing and Materials, pp. 137-150, 1994.
20. K. P. Menard, *Dynamic Mechanical Analysis: A Practical Introduction*, CRC Press, 1999.
21. M. S. Khalil, "The role of $BaTiO_3$ in modifying the dc breakdown strength of LDPE", IEEE Trans. Dielectr. Electr. Insul., Vol. 7, pp. 261-268, 2000.
22. M. M. Ueki and M. Zanin, "Influence of additives on the Dielectric Strength of High-density Polyethylene", IEEE Trans. Dielectr. Electr. Insul., Vol. 6, pp. 876-881, 1999.
23. A. J. Peacock, *Handbook of Polyethylene: Structures, Properties and Applications*, Marcel Dekker, New York, 2000.
24. J. D. Ferry, *Viscoelastic Properties of Polymers*, 3rd Ed, John Wiley and Sons, NY, 1980.
25. K. Lichtenecker and K. Rother; "Die Herleitung des logarithmischen Mischungsgesetzes als allegemeinen Prinzipien der staionaren Stromung", Phys. Zeit., Vol. 32, pp. 255-260, 1931.
26. J. C. Maxwell-Ganet, "Colours in metal glasses and metallic films", Philos. Trans. Roy. Soc., London, Ser. A 203, pp. 385-420, 1904.
27. L. D. Landau and E. M. Lifshitz, *Electrodynamics of Continuous Media*, 2nd Ed., Pergamon Press, Oxford, 1984.
28. Z. W. He, C. M. Zhen, X. Q. Liu, W. Lan, D. Y. Xu, and Y. Y. Wanget, "Microstructural characterization of low dielectric silica xerogel film", Thin Solid Films, Vol. 462-463, pp. 168-171, 2004.
29. T. Tepper and S. Berger, "Correlation between microstructure, particle size, dielectric constant, and electrical resistivity of nano-size amorphous SiO2 powder", Nanostructured Materials, Vol. 11, pp. 1081-1089, 2000.
30. L. K. H. van Beek, "Dielectric behavior of heterogeneous systems", in *Progress in Dielectrics*, Vol. 7, Heywood, London, UK, 1967.
31. L. A. Dissado and R. M. Hill, "Anomalous low frequency dispersion: A near DC conductivity in disordered low dimensional materials", J. Chem. Soc. Faraday Trans. II 80, pp. 291-319, 1984.
32. T. J. Lewis, "Interfaces are the Dominant Feature of Dielectrics at the Nanometric Level", IEEE Trans. Dielectr. Electr. Insul., Vol. 11, pp. 739-753, 2004.
33. C. T. O'Konski, "Electric Properties of Macromolecules, V.: Theory of Ionic Polarization in Polyelectrolytes", J. Phys. Chem., Vol. 64, pp. 605-619, 1960.
34. A. K. Jonscher, *Dielectric Relaxation of Solids*; Chelsea Dielectric Press, 1983.
35. A. P. Legrand, H. Hommel, A. Tuel, A. Vidal, H. Balard, E. Papirer, P. Levitz, M. Czernichowski, R. Erre, H. Van Damme, J. P. Gallas, J. F., Hemidy, J. C., Lavalley, O. Barres, A. Burneau, and Y. Grillet, "Hydroxyls of silica powders", Advances in Colloid and Interface Science, Vol. 33, Issues 2-4 , pp. 91-330, 1990.
36. M-I, Baraton, "FTIR Surface Spectrometry of Nano-sized Particles", *Handbook of Nanostructured Materials and Nanotechnology*, Eds. H. S. Nalwa, Vol. 2, Academic Press, NY, 2000
37. C. P. Pool, *Electron Spin Resonance*, Wiley, NY, 1983.

38. M. Bersohn, and J. C. Baird, *An Introduction to Electron Paramagnetic Resonance*, W. A. Benjamin, Inc., 1966.

39. M. R. Alexander, R. D. Short, F. R. Jones, W. Michaeli, and J. C. Blomfield, "A study of HMDSO/O_2 plasma deposits using a high-sensitivity and –energy resolution XPS instrument: curve fitting of the Si 2p core level", Applied Surface Science, Vol. 137, pp. 179-183, 1999.

40. J. H. Scofield, "Hartree-Slater subshell photoionization cross-sections at 1254 and 1487 eV", J. of Elect. Spect. and Related Phenomena, Vol. 8, pp. 129-137, 1976.

41. B. Lucíla and M. Fiolhais, "Energetics of charge distributions", Eur. J. Phys., Vol. 23, pp. 427-431 2002.

42. G. Pacchioni, A. Ferrari, and G. Ieranò, "Cluster model calculations of oxygen vacancies in SiO_2 and MgO: Formation energies, optical transitions and EPR spectra", Faraday Discuss., Vol. 106, pp. 155-172, 1997.

43. M. Schwartz and R. J. Berry, "Ab initio investigation of substituent effects on bond dissociation enthalpies in siloxanes and silanols", J. Molecular Structure: THEOCHEM, Vol. 538, Issues 1-3, pp. 9-17, 2001.

44. C. C. Ku and R. Liepin, *Electrical Properties of Polymers: Chemical Principles*, Hanser Publishers, 1987.

45. J. K. Nelson and H. Sabuni, "The effects of plasticizer on the electric strength of polystyrene", J. Material Sc, Vol. 14, pp. 2791-2796, 1979.

46. T. Miyamoto and K. Shibayama, "Free-volume model for ionic conductivity in polymers", J. Appl. Phys., Vol. 44, No. 12, pp 5372-76, 1973.

47. J. Artbauer; "Electric strength of polymers", J. Phys. D: Appl. Phys., Vol. 29, pp. 446-456, 1996.

48. A. H. Otto, D. Prescher, E. Gey, and S. Schraderet, "Proton affinities of some polyfluoroalkanes in comparison to the unsubstituted alkanes"; J. Fluorine Chem., Vol. 82, pp. 55-71, 1997.

49. D. Bamford, M. Jones, J. Latham, R. J. Hughes, M. A. Alam, J. Stejny, and G. Dlubeket, "Anisotropic Nature of Open Volume "Defects" in Highly Crystalline Polymers", Macromolecules, Vol. 34, pp. 8156-8159, 2001.

50. G. Dlubek, J. Stejny, Th. Lüpke, D. Bamford, K. Petters, Ch. Hübner, M. A. Alam, and M. J. Hillet, "Free-volume variation in polyethylenes of different crystallinities: Positron lifetime, density, and X-ray studies", Journal of Poly. Sc. Part B, Poly. Phys., Vol. 40, pp. 65-81, 2002.

51. L. A. Dissado and J. C. Fothergill, *Electrical degradation and breakdown in polymers*, Peter Peregrinus Ltd., 1992.

52. M. Ieda, M. Nagao, and M. Hikita, "High-field Conduction and Breakdown in Insulating Polymers", IEEE Trans. Dielectr. Electr. Insul., Vol. 1, pp. 934-945, 1994.

53. S. S. Sternstein and A. J. Zhu, "Reinforcement mechanism of nanofilled polymer melts as elucidated by nonlinear viscoelastic behavior", Macromolecules, Vol. 35, No. 19, pp. 7262-7273, 2002.

J. Keith Nelson (F'90) was born in Oldham, UK and received his B.Sc.(Eng.) and Ph.D. degrees from the University of London, UK. He is currently Philip Sporn Chair of Electric Power Engineering at the Rensselaer Polytechnic Institute. Prior to his appointment at Rensselaer, he was manager of Electric Field Technology Programs at the General Electric R &D Center in Schenectady, NY. He has held numerous IEEE appointments including that of the Presidency of the Dielectrics & Electrical Insulation Society, 1995-6. He is a chartered electrical engineer, a Fellow the IEE and the recipient of the IEEE Millennium Medal.

Clive W Reed (M'80) graduated from the University of Bristol, England in 1956 with a First Class Special Honors B.Sc. degree in organic chemistry and with a Ph.D. degree in physical chemistry in 1960. After a postdoc in low temperature physics at NRC in Ottawa, Canada, in 1963 he joined GE Corporate Research and Development, Schenectady, NY, where he worked on hv insulation and dielectric phenomena for numerous commercial applications until retirement in 2002. He is past chairman of CEIDP, past member of NAS-NRC's Committee on Dielectrics, past chairman of CIGRE's Committee on Materials for Electro-technology, and has served in many capacities for these and other professional organizations and on NIST, US Government, and industrial review and advisory committees. Presently, he is an independent consultant on dielectrics and HV insulating materials and design.

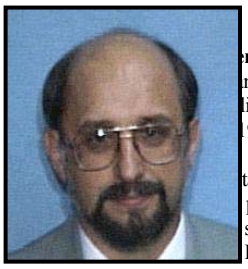

r Zenger is Technical Leader, Underground Trans-mission and nager of the EPRI Cable Testing Network (ECTN) in the Power livery Sector of the Electric Power Research Institute. He joined EPRI 996 as a project manager for cable systems and presently is engaged in development of ECTN Transmission a cable test facility for high tage cables at the Lenox lab. He was employed for seventeen years in power cable industry in the US and Germany. Prior to that he worked seven years at two German utilities. Walter Zenger received his degree Electrical Engineering (Power Engineering) from Fachhochschule Munich, Germany in 1972. He is a Member of IEEE Power Engineering Society, Insulated Conductors Committee, and CIGRE. He is US representative of CIGRE Study Committee B1 – Cable Systems and North American representative of its Customer Advisory Group.

Robert J. Keefe earned a B.Sc. degree in chemical engineering from the University of Wisconsin–Madison and an MBA from Indiana University's Kelley School of Business. He is currently the manager of Underground Distribution for the Electric Power Research Institute (EPRI) in Palo Alto, CA. He is also currently the Chair of the IEEE Insulated Conductor Committee discussion group on characteristics of insulating materials (ICC-AID). Prior to joining EPRI in 2001, he had worked at General Cable, BICC, and BP Chemicals. There, he had a combined 15 years experience working in materials technology, developing polymeric compounds and manufacturing processes for dielectric and semi-conductive applications.

Linda S. Schadler was born in Niskayuna, NY and received the B.S. degree from Cornell University and the Ph.D. degree from the University of Pennsylvania in Materials Science and Engineering. She is currently a Professor of Materials Science and Engineering at Rensselaer Polytechnic Institute. Prior to her appointment at Rensselaer, she taught at Drexel University. She is currently a member of the National Materials Advisory Board and a member of the TMS, Mining Metals and Materials Advisory Board.

Mihir Roy is presently a graduate student in Rensselaer Polytechnic Institute at Troy, and working in 'Nano-dielectrics' group.